

Frequency-dependent anisotropy due to fluid flow in bed limited cracks

S. R. Tod

Department of Applied Mathematics and Theoretical Physics, University of Cambridge, Silver Street, Cambridge, CB3 9EW, UK

E. Liu

British Geological Survey, Murchison House, West Mains Road, Edinburgh, EH9 3LA, UK

Abstract. Evidence from a number of measurements support the idea that anisotropy, or shear-wave splitting, exhibits a frequency dependence. This is generally attributed to properties of the microstructure of the rock and typically assumed to be the result of scattering from oriented inclusions within the rock mass. However, there are a number of competing mechanisms that may give rise to this observed frequency dependence. The scale length of the inclusions must be much smaller than the wavelength at which the measurements were conducted, in order for their presence to be observed as an effective anisotropy, and may therefore be insufficient to account for a significant frequency dependence. An alternative mechanism resulting in frequency dependence is the transfer of fluid between the inclusions, assumed to be fluid filled. Using an established model, it is demonstrated that this fluid effect is potentially significant enough to explain observed frequency dependence.

1. Introduction

There is evidence from measurements taken from a range of experiments that shear wave splitting exhibits a frequency dependence (e.g., Marson-Pidgeon and Savage, 1997; Lynn et al., 1999). Marson-Pidgeon and Savage (1997) and Matcham et al. (2000), see Figure 1, indicate that oriented inclusions are the most likely cause of the observed results in the earthquake data, and the seismic data of Lynn et al. (1999) and Liu et al. (2002), see Figure 2, is modeled by Chesnokov et al. (2001) in terms of scattering from such. To achieve results in the modeling comparable to those from the data it was found necessary to use a high concentration of large inclusions. These values are at levels close to, or beyond, the range of validity of effective medium theories.

Effective medium theories have been developed that give the overall properties of an elastic material containing cracks by a number of authors (e.g., O’Connell and Budiansky, 1974; Hudson, 1980). These typically require the description of a mean crack shape. In general, for simplicity, this is taken to be a flat circular (“penny-shaped”) crack, though it may also be elliptical (Budiansky and O’Connell, 1976). However, these restrictions place an unnecessary limitation on the theory, when it is perhaps more realistic to describe

a crack in terms of a bounded width and an otherwise ellipsoidal shape. Such ellipsoids of non-zero thickness have been shown to give rise to more general formulations (e.g., Kuster and Toksöz, 1974; Hudson, 1994) and non-elliptical thin cracks have also been studied (e.g., Mavko and Nur, 1978).

A generalization of the method of smoothing (Hudson, 1994) has been used to study the role of the crack width and the ratio of the two larger dimensions in determining the properties of the effective medium. This results in an orthorhombic medium, and provides a suitable description of a material where the crack dimensions are restricted in one direction due to, for example, bed-limiting effects, while remaining unconfined in other directions. In addition to the isolated crack description, the theory is extended to include the fluid flow mechanism of Tod (2001) that models the flow as being dominated by crack to crack flow and is valid for low matrix porosities over a large range of frequencies, provided that the wavelength is much greater than the crack dimensions. The resulting theory predicts a frequency dependence in the elastic stiffnesses as a result of the effects of fluid flow.

2. Data Interpretation

The broadband earthquake data from New Zealand, shown in Figure 1, covers a range of frequencies below 0.1 Hz. The original figure given by Marson-Pidgeon and Savage (1997) was of time delay against period, while we have replotted the data against frequency. While the large errors bars at low frequency leave the interpretation a little fragile there is a clear decrease in delay time with frequency, of a roughly linear nature, with perhaps the suggestion of a peak, non-zero, frequency before a slight decrease for the lowest frequencies.

The VSP from the Bluebell-Altamont Field, Utah, shows a limited coverage of the seismic frequency range and the three data points given by Chesnokov et al. (2001) suggest a monotonic decrease in shear wave splitting with frequency, so that maximum anisotropy is attained in the static limit, in agreement with the scattering theory. A more comprehensive analysis of the same data by Liu et al. (2002), shown in Figure 2, suggests that this trend is perhaps not quite so simple. While one may question, due to the limited frequency coverage of the data, the two points that buck the aforementioned trend, there is a possible suggestion that the maximum anisotropy is achieved at a low, non-zero, frequency and that the behavior at high frequencies is not quite as simple as it might at first seem.

Copyright by the American Geophysical Union.

Paper number .
0094-8276/02/\$5.00

3. Theory

The effective medium theory due to Hudson (1980) and based on the method of smoothing (Keller, 1964), was extended by Hudson (1994) to include cracks of finite width, modeled as ellipsoids with semi-axis a , b and c . The elastic stiffnesses \mathbf{c} of the resulting effective medium for a single set of aligned cracks of identical dimensions are of the form

$$\mathbf{c} = \mathbf{c}^0 + s\mathbf{c}^+\mathbf{E}, \quad (1)$$

where \mathbf{c}^0 are the elastic stiffnesses of the isotropic matrix material, $s = 4\pi\nu^s abc/3$ is the volume fraction of cracks, which we may identify as the porosity of the cracks, in terms of the number density ν^s ,

$$\mathbf{c}^+ = \mathbf{c}' - \mathbf{c}^0 \quad (2)$$

in terms of the elastic stiffnesses of the inclusions \mathbf{c}' , and \mathbf{E} is defined in terms of the Eshelby (1957) tensor \mathbf{S} as

$$\mathbf{E} = (\mathbf{S}\mathbf{s}^0\mathbf{c}^+ + \mathbf{I})^{-1}, \quad (3)$$

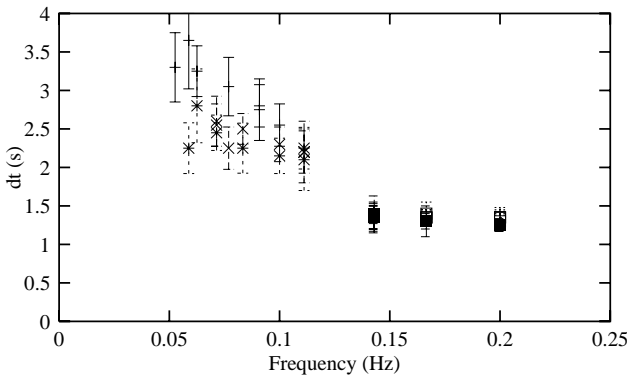


Figure 1. Delay time as a function of frequency for three SKS and two ScS events recorded at a broadband station in Wellington, New Zealand. Data reproduced with permission from K. Marson-Pidgeon and M. K. Savage, from Figure 4 of Marson-Pidgeon and Savage (1997), originally displayed as a function of period.

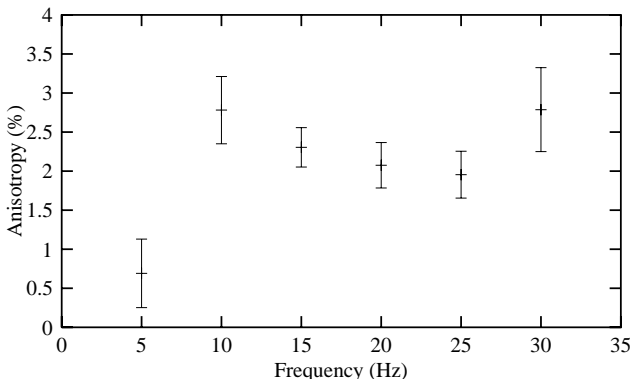


Figure 2. The variation in shear wave anisotropy with frequency from a VSP in the Bluebell-Altamont Field, Utah. Data reproduced with permission from H. Lynn, Lynn Inc.

where \mathbf{s}^0 are the elastic compliances of the matrix material and \mathbf{I} is the identity tensor. \mathbf{c} corresponds to an orthorhombic medium. For multiple crack sets, the perturbation to the background stiffnesses \mathbf{c}^0 can be found by summing over contributions from each of the sets. \mathbf{E} relates the strain in an inclusion \mathbf{e} to the imposed strain at infinity \mathbf{e}^0 ,

$$\mathbf{e} = \mathbf{E}\mathbf{e}^0. \quad (4)$$

The effective density of the medium is

$$\rho = \rho^0(1-s) + \rho's, \quad (5)$$

where ρ^0 and ρ' are the density of the matrix and inclusion respectively.

To determine the strain in an inclusion due to an imposed stress at infinity $\boldsymbol{\sigma}^0$ and a fluid pressure p_f within the inclusion we write, following Tod (2002b),

$$\mathbf{e} = \hat{\mathbf{E}}\mathbf{e}^0 \quad (6)$$

where

$$\hat{E}_{ijkl} = \bar{E}_{ijkl} + \left(\bar{E}_{ijrs}s_{rspp}^0 - \frac{\delta_{ij}}{3\kappa} \right) H_{mn}c_{mnkl}^0, \quad (7)$$

with

$$\bar{\mathbf{E}} = (\mathbf{I} - \mathbf{S})^{-1} \quad (8)$$

the result for dry cracks, κ the bulk modulus of the matrix material and \mathbf{H} arising from a linearized relation of the form

$$p_f = H_{ij}\sigma_{ij}^0 \quad (9)$$

derived from the fluid flow model of Hudson et al. (1996) and Tod (2001), and given explicitly by Tod (2002b), valid for low matrix porosities.

On the assumption that the cracks are all fully aligned and are of identical dimension we may write (Tod, 2002b)

$$\hat{E}_{ijkl} = \bar{E}_{ijkl} + \frac{\kappa_f}{3\kappa} (\bar{E}_{ijuu} - \delta_{ij}) \chi \bar{E}_{vvkl}, \quad (10)$$

where

$$\chi = \frac{1}{1 - i\omega\tau\gamma} \left[i\omega\tau - \frac{1}{\gamma + i\omega\tau K_2(1 - i\omega\tau\gamma)} \right], \quad (11)$$

$$\gamma = 1 - \frac{\kappa_f}{\kappa} + \frac{\kappa_f}{3\kappa} \bar{E}_{ijij}, \quad (12)$$

and

$$K_2 = \frac{\kappa_f K^r}{sv^2\tau\eta_f} \quad (13)$$

for an isotropic *in situ* rock permeability K^r , after Tod (2002a). κ_f and η_f are the bulk modulus and viscosity of the fluid, v is taken to be a lowest order approximation to the wavespeed, and τ is a relaxation parameter that characterizes the time-scale of pressure equalization between neighboring cracks. Hudson et al. (1996) estimate this to be

$$\tau = \frac{\phi^m \eta_f l^2}{\kappa_f K^m} \quad (14)$$

in terms of a characteristic length scale l , which we may associate with a crack separation distance, the matrix permeability K^m and the matrix porosity ϕ^m , both the result of lab measurements on core samples. For the modeling that follows, we replace \mathbf{E} in equation (1) with $\hat{\mathbf{E}}$ (equation (10)).

4. Modeling Results

We start by attempting to reproduce the behavior shown in the VSP data in Figure 2. We model the properties of the matrix material as $v_P = 4.88 \times 10^3 \text{ m s}^{-1}$, $v_S = 2.68 \times 10^3 \text{ m s}^{-1}$ and $\rho = 2.55 \times 10^3 \text{ kg m}^{-3}$ and take the inclusions to be filled with gas with $v_P = 0.64 \times 10^3 \text{ m s}^{-1}$ and $\rho = 0.18 \times 10^3 \text{ kg m}^{-3}$, as Chesnokov et al. (2001). Furthermore, we know from Lynn et al. (1999) that $K^m < 1.0 \times 10^{-15} \text{ m}^2$ and $\phi^m < 0.08$, and we take $\eta_f = 1.8 \times 10^{-5} \text{ kg m}^{-1} \text{ s}^{-1}$ for the gas. The parameters still available to us are the *in situ* rock permeability, the pressure relaxation time, the volume fraction of cracks, two aspect ratios that describe the shape of the crack and up to three Eulerian angles describing the orientation of the cracks. We estimate $K^r = 2.6 \times 10^{-11} \text{ m}^2$ and $\tau = 1.0 \times 10^{-3} \text{ s}$ and use the following values: $s = 4.7 \times 10^{-5}$, $\alpha \equiv c/a = 1.0 \times 10^{-5}$, $\beta \equiv b/a = 2.5 \times 10^{-2}$ and position the crack normal in the (1, 3)-plane at 60° to the vertical. If we describe the (shear wave) anisotropy by

$$\gamma_T = \frac{v_S^{\text{fast}} - v_S^{\text{slow}}}{v_S^{\text{fast}}} \quad (15)$$

then the change in anisotropy with frequency due to the vertical incidence is given in Figure 3. This shows the same qualitative behavior as Figure 2, with a decrease in

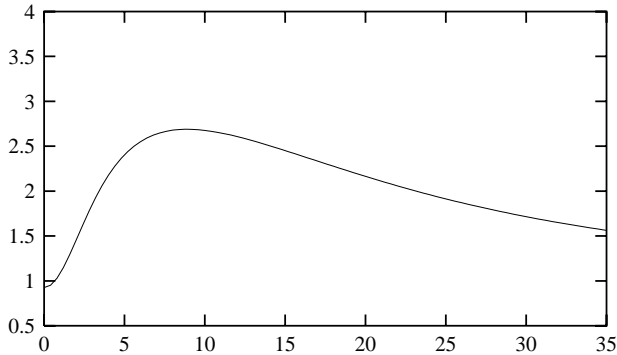


Figure 3. Modeling the change in shear wave anisotropy with frequency from the VSP at Bluebell-Altamont Field, Utah. See text for material parameters.

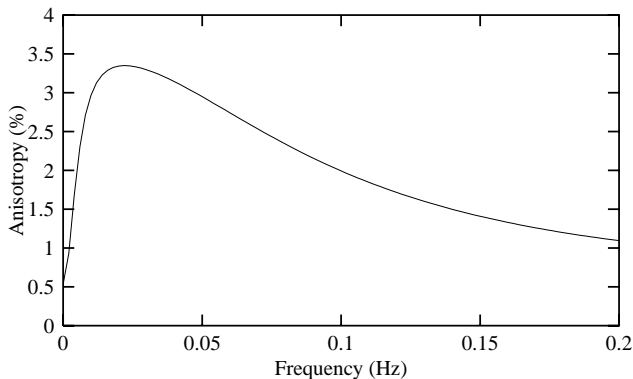


Figure 4. Modeling the change in shear wave anisotropy with frequency from the broadband data at Wellington, New Zealand. See text for material parameters.

anisotropy with frequency from a peak value at around 8 Hz. The data point at 30 Hz, with by far the largest error bar, cannot be explained by the model, though it goes against intuition.

From the value of τ we can calculate two length scales for the problem. With a shear wave speed of $v_S = 2.68 \times 10^3 \text{ m s}^{-1}$ in the matrix material we have a length scale for pressure equalization of 2.7 m, while using the estimate for τ (equation (14)) we have an approximate to the average crack separation distance of $l = 7.2 \times 10^{-3} \text{ m}$. Now, as a first approximation, the crack number density is given by $\nu^s = l^{-3}$, with which, together with the values of s , α and β used above, we can estimate the longest crack dimension to be $a = 2.6 \times 10^{-2} \text{ m}$.

Rather less is known about the *in situ* measurements appropriate to the earthquake data reproduced in Figure 1, we may nevertheless aim to achieve a qualitative comparison. Using the same rock properties, but switching to a fluid, such that $v_P = 1.5 \times 10^3 \text{ m s}^{-1}$ and $\rho = 1.0 \times 10^3 \text{ kg m}^{-3}$ then using $s = 3.1 \times 10^{-4}$, $\alpha = 1.0 \times 10^{-4}$, $\beta = 3.5 \times 10^{-2}$, $\tau = 5.0 \times 10^{-2} \text{ s}$ and $\eta_f/K^r = 1.0 \times 10^3 \text{ kg m}^{-3} \text{ s}^{-1}$, the modeling yields Figure 4. This shows the same qualitative behavior as Figure 1 with the anisotropy drop occurring over the same frequency and being of the same order of magnitude.

While the volume fraction s is present in the non-dimensional parameter K_2 (equation (13)) that influences both the frequency at which the peak anisotropy occurs and the magnitude of the peak in comparison with the high frequency limiting value, its major effect is simply to scale the magnitude of the anisotropy. τ also influences both the location and magnitude of the peak. Changes in the two aspect ratios alter the magnitude of the resulting anisotropy, but has little or no effect on the shape of the variation of the anisotropy with frequency. On the assumption that there is only a single set of aligned cracks present, we may recover the crack orientation from P-wave AVOA analysis of wide azimuth data.

5. Conclusions

We have presented a model that describes a fluid flow mechanism between ellipsoidal cracks that produces a frequency dependence in the resulting effective material parameters and hence in the shear wave splitting. The model has been used to simulate field observations of frequency dependence in both exploration and earthquake data sets, with great success and has been used to provide estimates of otherwise unknown quantities, the *in situ* rock permeability and the crack dimensions. We demonstrate that the effects of fluid flow, whether that be gas or liquid, are non-negligible and an important contributing factor to observed frequency dependent anisotropy. While in general the effects of both fluid flow and scattering need to be taken into account when interpreting the frequency dependence, the effect is likely to be dominated by one process or the other dependent upon scaling arguments.

Acknowledgments. We would like to thank Katrina Marson-Pidgeon and Martha K. Savage for providing us with the data from Figure 4 of Marson-Pidgeon and Savage (1997), reproduced in Figure 1, Heloise Lynn, Lynn Inc., for permission to use data from a 9C VSP in the Bluebell-Altamont Field, Utah, reproduced in Figure 2, John A. Hudson at DAMTP, University of Cambridge for support and encouragement and John H.

Queen, Conoco, for useful discussion. The work was sponsored by the Natural Environment Research Council through project GST022305, as part of the thematic programme *Understanding the micro-to-macro behaviour of rock fluid systems ($\mu 2M$)* and is published with the approval of the Executive Director of the British Geological Survey (NERC).

References

- Budiansky, B., and R. J. O'Connell, Elastic moduli of a cracked solid, *Int. J. Solids Struct.*, **12**, 81–97, 1976.
- Chesnokov, E. M., J. H. Queen, A. A. Vichorev, H. B. Lynn, J. M. Hooper, I. O. Bayuk, J. A. Castagna, and B. Roy, Frequency dependent anisotropy, in *71st Ann. Mtg. SEG, Exp. Abs.*, San Antonio, 2001.
- Eshelby, J. D., The determination of the elastic field of an ellipsoidal inclusion and related problems, *Proc. R. Soc. Lond. A*, **241**, 376–396, 1957.
- Hudson, J. A., Overall properties of a cracked solid, *Math. Proc. Camb. Phil. Soc.*, **88**, 371–384, 1980.
- Hudson, J. A., Overall properties of materials with inclusions or cavities, *Geophys. J. Int.*, **117**, 555–561, 1994.
- Hudson, J. A., E. Liu, and S. Crampin, The mechanical properties of materials with interconnected cracks and pores, *Geophys. J. Int.*, **124**, 105–112, 1996.
- Keller, J. B., Stochastic equations and wave propagation in random media, *Proc. Symp. Appl. Math.*, **16**, 145–170, 1964.
- Kuster, G. T., and M. N. Toksöz, Velocity and attenuation of seismic waves in two-phase media: Part 1. Theoretical formulations, *Geophysics*, **39**, 587–606, 1974.
- Liu, E., J. H. Queen, X. Y. Li, M. Chapman, H. B. Lynn, and E. M. Chesnokov, Analysis of frequency-dependent seismic anisotropy from a multicomponent VSP, 2002, proc. 10th International Workshop on Seismic Anisotropy, *J. Appl. Geophys.*, submitted.
- Lynn, H. B., W. E. Beckham, K. M. Simon, C. R. Bates, M. Layman, and M. Jones, P-wave and S-wave azimuthal anisotropy at a naturally fractured gas reservoir, Bluebell-Altamont Field, Utah, *Geophysics*, **64**, 1312–1328, 1999.
- Marson-Pidgeon, K., and M. K. Savage, Frequency-dependent anisotropy in Wellington, New Zealand, *Geophys. Res. Lett.*, **24**, 3297–3300, 1997.
- Matcham, I., M. K. Savage, and K. R. Gledhill, Distribution of seismic anisotropy in the subduction zone beneath the Wellington region, New Zealand, *Geophys. J. Int.*, **140**, 1–10, 2000.
- Mavko, G. M., and A. Nur, The effect of nonelliptical cracks on the compressibility of rocks, *J. Geophys. Res.*, **83**, 4459–4468, 1978.
- O'Connell, R. J., and B. Budiansky, Seismic velocities in dry and saturated cracked solids, *J. Geophys. Res.*, **79**, 5412–5426, 1974.
- Tod, S. R., The effects on seismic waves of interconnected nearly aligned cracks, *Geophys. J. Int.*, **146**, 249–263, 2001.
- Tod, S. R., The effects of stress and fluid pressure on the anisotropy of interconnected cracks, *Geophys. J. Int.*, **149**, 149–156, 2002a.
- Tod, S. R., Bed-limited cracks in effective medium theory, 2002b, *Geophys. J. Int.*, in review.

S. R. Tod, Department of Applied Mathematics and Theoretical Physics, University of Cambridge, Silver Street, Cambridge, CB3 9EW, UK. (s.r.tod@damtp.cam.ac.uk)

E. Liu, British Geological Survey, Murchison House, West Mains Road, Edinburgh, EH9 3LA, UK. (e.liu@bgs.ac.uk)

(Received _____.)